Electronic Supplementary Material (ESI) for Materials Advances.
This journal is © The Royal Society of Chemistry 2021

Supporting Information

DFT Calculations: DFT/TD-DFT calculations were carried out using the B3LYP hybrid functional and the 6-311+G(d,p) basis set in the GAUSSIAN09 software package. Alkyl chains were replaced with a methyl group to simplify calculations and reduce computational time. Structures were optimized, and a frequency analysis was performed. *Transfer Integrals:* Electron transfer integrals (LUMO – LUMO overlap, B3LYP/6-31G(d)) for molecular pairs from crystal structures of **2,7-dihexyl-diFIDT-di(N(CN))** and **3,8-dihexyl-diFIDT-di(N(CN))** were calculated using the approach of Valeev et al. with Gaussian 16 Rev A.03 software.[2] *Symmetry Adapted Perturbation Theory (SAPT0) calculations:* Symmetry adapted perturbation interaction energies (SAPT0/jun-cc-pvdz) were calculated for molecular pairs from crystal structures using Psi4 software. In each case, H and F atoms were first allowed to relax geometrically to allow for error in positioning hydrogen atoms from x-ray diffraction data, and to allow the in silico substitution of H and F atoms. Total SAPT0 energies (TOT) are decomposed into electrostatic (ES, Keesom interaction), exchange (EX, Pauli repulsion), induction (IND, Debye interaction) and dispersion (DISP, London interaction) energies. All energies are in kcal/mol.

Characterization: ^{1}H, ^{19}F, and ^{13}C NMR spectra were recorded on a Bruker AV-400 (400 MHz), referenced using the residual solvent resonance of chloroform-d, DMSO-d_6 or 1,1,2,2-tetrachloroethane-d_2 and are given in ppm. Electrospray mass spectrometry was performed with a Waters LCT Premier (ES-ToF) mass spectrometer. UV–vis spectra were recorded on a UV-1800 Shimadzu UV–vis spectrometer. TGA measurements, using ≥ 2 mg of material, were conducted under nitrogen between 25 and 600 °C at a scan rate of 10 °C min^{-1} with a Mettler Toledo TGA/DSC 1LF/UMX instrument. DSC measurements, using ~3 mg of material, were conducted under nitrogen at a scan rate of 10 °C min^{-1} with a TA DSC-Q20 instrument. The melting temperature (T_m) was extracted from the DSC data as the extrapolated onset temperature of the major endotherm of the 1st heating cycle if stated. Cyclic voltammograms were recorded using a Metrohm Autolab PGStat101. The experimental setup consisted of an Ag/Ag+ reference electrode, a platinum wire counter electrode and a platinum working electrode, and all measurements were carried out under nitrogen at room temperature. Measurements were performed in anhydrous, degassed solutions of CH_2Cl_2 with tetrabutylammonium hexafluorophosphate (0.1 M) electrolyte. After each measurement, an arbitrary amount of ferrocene was added to the solution as an internal reference.

Single Crystal Growth and Analysis: Small molecule solutions in chlorobenzene (0.5 mg in 0.75 mL) were placed in 2 mL glass vials. These vials were placed into larger vials containing methanol (2.5 mL) which were then sealed. Equilibration via vapour diffusion occurred over 3 to 5 days, after which crystals were analysed. Details of the structural determinations can be found below.

Device Fabrication and Characterisation: All film preparation and characterisation steps were carried out under inert atmosphere. Organic thin film transistors (OTFTs) were fabricated in bottom-contact top-gate (BC – TG) configuration. The Al/Au (5 nm/35 nm) source and drain electrodes were vapour-deposited using shadow mask on the glass substrate. The small molecule solution (5 mg mL^{-1} in chlorobenzene) was blade coated on the substrates at 100 °C with the blade speed of 50 mm s^{-1} and then the substrates were kept at 100 °C for 5 mins. ~900 nm CYTOP film was deposited on top of the semiconductor by spin coating at 2000 rpm spin rate followed by annealing at 50 °C for 1 hr. The capacitance of the CYTOP dielectric was measured 2.1 nF cm^{-2}. 70 nm Al was vapour-deposited at the top as the gate electrode. The current-voltage characteristics for the devices were measured using KEYSIGHT B2912A Precision Source/Measure Unit.

Experimental

*2,2'-(5,10-Difluoro-2,7-dihexyl-s-indaceno[1,2-b:5,6-b']dithiophene-4,9-diylidene)dicyanoimine (**2,7-dihexyl-diFIDT-di(N(CN))**):* To solution of 5,10-difluoro-2,7-dihexyl-s-indaceno[1,2-b:5,6-b']dithiophene-4,9-dione[1] (200 mg, 0.4 mmol) in anhydrous DCM (20 mL) at 0 °C was added $TiCl_4$ (0.44 mL, 4 mmol) dropwise. The resulting mixture was stirred for 10 mins at 0 °C. To this was added dropwise a solution bis(trimethylsilyl)carbodiimide (0.91 mL, 4 mmol) in anhydrous DCM (5 mL). The mixture was allowed to warm to room temperature and stirred for 4 hrs to give a deep red mixture. Another portion of $TiCl_4$ (0.22 mL, 2 mmol) and bis(trimethylsilyl)carbodiimide (0.45 mL, 2 mmol) were added and the mixture was allowed to stir overnight. TLC (2/1 petroleum ether/DCM) confirmed the reaction was complete. Water was added (100 mL) and the mixture was extracted with chloroform (2 x 50 mL). The combined organic extracts were rinsed with water (2 x 50 mL) and brine (50 mL), dried over anhydrous sodium sulfate, filtered and concentrated under reduced pressure. The crude solid was triturated with methanol, filtered, washed with further methanol and acetone, then dried in vacuo to give a dark coloured, crystalline solid (110 mg, 50 %). m.p. N/A. ^1H NMR (400 MHz, $CDCl_3$, δ): 7.36 (s, 2 H, ArH), 2.82 (t, $^3J = 7.7$ Hz, 4 H, CH_2), 1.70 (m, 4 H, CH_2), 1.45-12.5 (m, 12 H, CH_2), 0.90 (t, $^3J = 6.9$ Hz, 6 H, CH_3). ^{13}C NMR (126 MHz, TCE-*d₂*, 120 °C, δ): 173.97, 155.42, 147.67, 147.59 (d, $^1J = 270$ Hz, CF), 137.56, 129.93 – 129.45 (m, CF), 128.77 – 128.25 (m, CF), 119.61, 113.41, 31.08, 30.88, 30.55, 28.31, 22.09, 13.49. ^{19}F NMR (377 MHz, $CDCl_3$, δ): -124.30 (s, CF). IR (cm^{-1}) 2179 (C≡N), 1602 (C=N-R). HRMS (ES-TOF) m/z: $[M]^+$ calcd. for $C_{30}H_{28}F_2N_4S_2$, 546.1723; found, 546.1734.

*Diethyl 2,5-difluoro-3,6-bis(4-hexylthiophen-2-yl)terephthalate (**[3]**):* A mixture of 2,5-dibromo-3,6-difluoroterephthalic acid diethyl ester[1] ***([1])*** (2.9 g, 6.97 mmol) and (4-

hexylthiophen-2-yl)trimethylstannane *([2])* (5.30 g, 16 mmol) in anhydrous DMF (80 mL) were degassed for 45 mins. Tetrakis(triphenylphosphine)palladium(0) (584 mg, 0.51 mmol, 0.07 equiv.) was added and the mixture degassed for a further 15 mins. The mixture was stirred at 100 °C for 17 hrs. The mixture was cooled to RT, diluted with DCM (100 mL) and the crude reaction mixture passed through a plug of 15 % KF in silica, eluting with DCM. The solvent was then concentrated in vacuo. DCM (150 mL) was added and the organic phase washed with water (4 x 100 mL) and brine (100 mL). The combined organics were dried over anhydrous magnesium sulfate, filtered and the solvent removed in vacuo. The crude product was purified by silica gel chromatography (petroleum ether 2:1 DCM). The product was collected and dried under vacuum to give diethyl 2,5-difluoro-3,6-bis(4-hexylthiophen-2-yl)terephthalate (3.38 g, 83 %) as a pale orange solid. ^{1}H NMR (400 MHz, $CDCl_3$, δ): 7.07 (d, ^3J = 1.5 Hz, 2 H, ArH), 7.04 (d, ^3J = 1.5 Hz, 2 H, ArH), 4.24 (q, ^3J = 7.5 Hz, 4 H, CH_2), 2.61 (t, ^3J = 7.5 Hz, 4 H, CH_2), 1.66 – 1.58 (m, 4 H, CH_2), 1.39 – 1.27 (m, 12 H, CH_2), 1.18 (t, ^3J = 7.2 Hz, 6 H, CH_3), 0.90 (t, ^3J = 6.9 Hz, 6 H, CH_3). ^{13}C NMR (101 MHz, $CDCl_3$, δ): 163.76, 152.07 (dd, ^1J = 252 Hz, ^4J = 4.5 Hz, CF), 143.62, 130.96, 130.81, 125.33 – 125.05 (m, CF), 123.07, 122.26 – 122.02 (m, CF), 62.43, 31.79, 30.56, 30.48, 29.06, 22.73, 14.19, 13.93. ^{19}F NMR (377 MHz, $CDCl_3$, δ): -119.73 (s, CF). HRMS (ES-TOF) m/z: $[M+H]^+$ calcd. for $C_{32}H_{41}O_4S_2F_2$, 591.2414; found, 591.2430.

2,5-Bis(4-hexylthiophen-2-yl)-3,6-difluoroterephthalic acid ([4]): Diethyl 2,5-difluoro-3,6-bis(4-hexylthiophen-2-yl)terephthalate *([3])* (4.9 g, 8.29 mmol) was suspended in ethanol (200 mL) and KOH (6.52 g, 116.12 mmol) was added as a single portion. The suspension was heated to reflux overnight. Upon heating a solution followed by a suspension was observed. The reaction was cooled to room temperature and aqueous hydrochloric acid (2.0 M, 250 mL) was added with stirring for 5 mins. The resulting precipitate was filtered, washed with plenty of water and dried in an oven at 140 °C to give 4.18 g (94%) of greenish solid. ^{1}H NMR (400

MHz, DMSO-d_6, δ): 14.17 (br s, 2 H, CO_2H), 7.42 (d, ^3J = 1.5 Hz, 2 H, ArH), 7.17 (d, ^3J = 1.5 Hz, 2 H, ArH), 2.59 (t, ^3J = 7.7 Hz, 4 H, CH_2), 1.63 – 1.55 (m, 4 H, CH_2), 1.35 – 1.25 (m, 12 H, CH_2), 0.86 (t, ^3J = 7.0 Hz, 6 H, CH_3). ^{13}C NMR (101 MHz, DMSO-d_6, δ): 164.33, 150.67 (dd, ^1J = 247 Hz, ^4J = 3.4 Hz, CF), 142.98, 130.86, 129.76, 125.69 – 125.38 (m, CF), 123.90, 120.43 – 120.16 (m, CF), 31.03, 29.86, 29.59, 28.32, 22.04, 13.92. ^{19}F NMR (377 MHz, DMSO-d_6, δ): -120.75 (s, CF). HRMS (ES-TOF) m/z: $[M+H]^+$ calcd. for $C_{28}H_{33}O_4S_2F_2$, 535.1788; found, 535.1794.

3,8-Dihexyl-5,10-difluoro-s-indaceno[1,2-b:5,6-b']dithiophene-4,9-dione ***(3,8-dihexyl-diFIDT-di(O))****:* 2,5-Difluoro-3,6-di-(4-hexylthiophen-2-yl-terephthalic acid ***([4])*** (4.0 g, 7.48 mmol) was suspended in anhydrous DCM (100 mL) and catalytic amount of anhydrous DMF (0.29 mL, 3.74 mmol). Thionyl chloride (10.90 mL, 149.62 mmol) was added dropwise over 15 minutes. The reaction was heated to reflux overnight. After cooling to room temperature, the solvent and thionyl chloride was removed under reduced pressure to give the acyl chloride an orange oil, which was used in the next step without further purification. The acyl chloride was redissolved in anhydrous DCM (100 mL) and then added dropwise to a suspension of anhydrous $AlCl_3$ (10.12 g) in DCM (100 mL) at 0 °C. The resultant mixture was allowed to warm to room temperature and stirred for 4 hrs. Aqueous hydrochloric acid (2.0 M, 400 mL) was added and the crude product extracted with chloroform (2 x 150 mL). The combined organic extracts were rinsed with water (2 x 150 mL) and brine (150 mL), dried over anhydrous sodium sulfate, filtered and concentrated under reduced pressure. The residue was reprecipitated in the minimum amount of hot DCM with methanol, filtered, washed with methanol and acetone then dried in vacuo to give a cyan blue solid (2.95 g, 78 %). m.p. 172 °C. ^1H NMR (400 MHz, $CDCl_3$, δ): 6.91 (s, 2 H, Ar H), 2.72 (t, ^3J = 7.7 Hz, 4 H, CH_2), 1.65 (m, 4 H, CH_2), 1.40-1.25 (m, 12 H, CH_2), 0.88 (t, ^3J = 6.8 Hz, 6 H, CH_3). ^{13}C NMR (101 MHz, $CDCl_3$, δ): 182.30, 152.21, 146.56 (dd, ^1J = 265 Hz, ^4J = 2.4 Hz, CF), 140.89, 139.04, 129.19

(m, CF), 128.30 (m, CF), 127.14, 31.70, 29.49, 29.07, 28.35, 22.73, 14.23. ^{19}F NMR (377 MHz, $CDCl_3$, δ): -129.64 (s, CF). IR (cm^{-1}) 1700 (C=O). HRMS (ES-TOF) m/z: [M]$^+$ calcd. for $C_{28}H_{28}F_2O_2S_2$, 498.1499; found, 498.1503.

*2,2'-(5,10-Difluoro-3,8-dihexyl-s-indaceno[1,2-b:5,6-b']dithiophene-4,9-diylidene)dicyanoimine (**3,8-dihexyl-diFIDT-di(N(CN))**):* To solution of 5,10-difluoro-3,8-dihexyl-s-indaceno[1,2-b:5,6-b']dithiophene-4,9-dione (200 mg, 0.4 mmol) in anhydrous DCM (20 mL) at 0 °C was added $TiCl_4$ (0.44 mL, 4 mmol) dropwise. The resulting mixture was stirred for 10 mins at 0 °C. To this was added dropwise a solution bis(trimethylsilyl)carbodiimide (0.91 mL, 4 mmol) in anhydrous DCM (5 mL). The mixture was allowed to warm to room temperature and stirred for 4 hrs to give a deep red mixture. Another portion of $TiCl_4$ (0.22 mL, 2 mmol) and bis(trimethylsilyl)carbodiimide (0.45 mL, 2 mmol) were added and the mixture was allowed to stir overnight. TLC (2/1 petroleum ether/DCM) confirmed the reaction was complete. Water was then added (100 mL) and the mixture was extracted with chloroform (2 x 50 mL). The combined organic extracts were rinsed with water (2 x 50 mL) and brine (50 mL), dried over anhydrous sodium sulfate, filtered and concentrated under reduced pressure. The crude solid was triturated with methanol, filtered, washed with further methanol and acetone then dried in vacuo to give a dark green, crystalline solid (112 mg, 51 %). m.p. 110 °C. ^{1}H NMR (400 MHz, $CDCl_3$, 50 °C, δ): 6.97 (2H, s, Ar H), 2.86 (4H, m, CH_2), 1.64 (4H, m, CH_2), 1.48-1.28 (12H, m, CH_2), 0.90 (6H, t, $^3J = 6.6$ Hz, CH_3). ^{13}C NMR (101 MHz, TCE-d_2, 120 °C, δ): 170.45, 150.71, 146.90 (d, $^1J = 267$ Hz, CF), 141.63, 138.89, 128.04, 112.31, 31.25, 29.55, 28.87, 28.41, 22.15, 13.54 (some carbon signals missing due to poor solubility). ^{19}F NMR (377 MHz, $CDCl_3$, 50 °C, δ): -100.00 (s, CF). IR (cm^{-1}) 2179 (C≡N). HRMS (ES-TOF) m/z: [M]$^+$ calcd. for $C_{30}H_{28}F_2N_4S_2$, 546.1723; found, 546.1714.

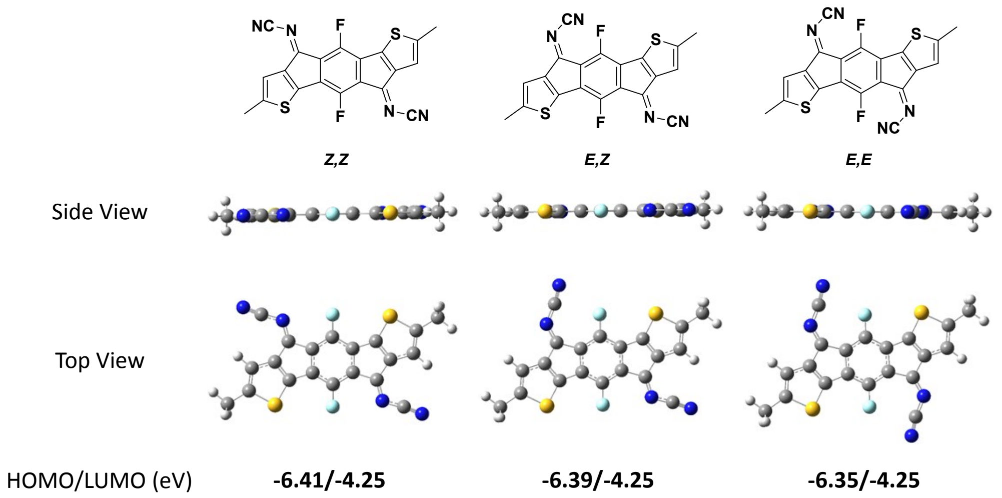

Figure S1: *Optimised structures for* ***diFIDT-di(C(CN))*** *isomers, calculated by DFT.*

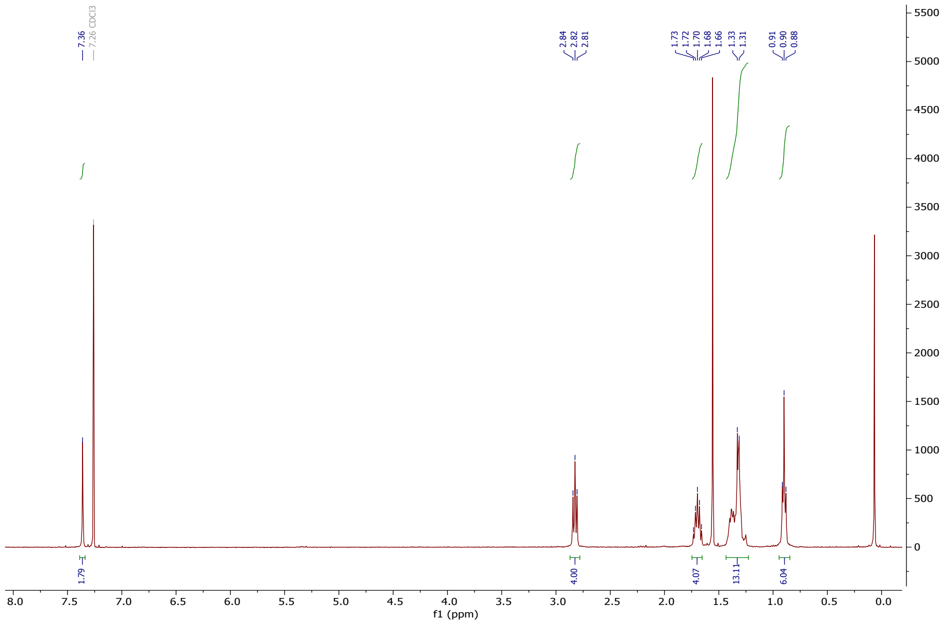

Figure S2: *^{1}H NMR of 2,2'-(5,10-difluoro-2,7-dihexyl-s-indaceno[1,2-b:5,6-b']dithiophene-4,9-diylidene)dicyanoimine (**2,7-dihexyl-diFIDT-di(N(CN))**) in CDCl$_3$.*

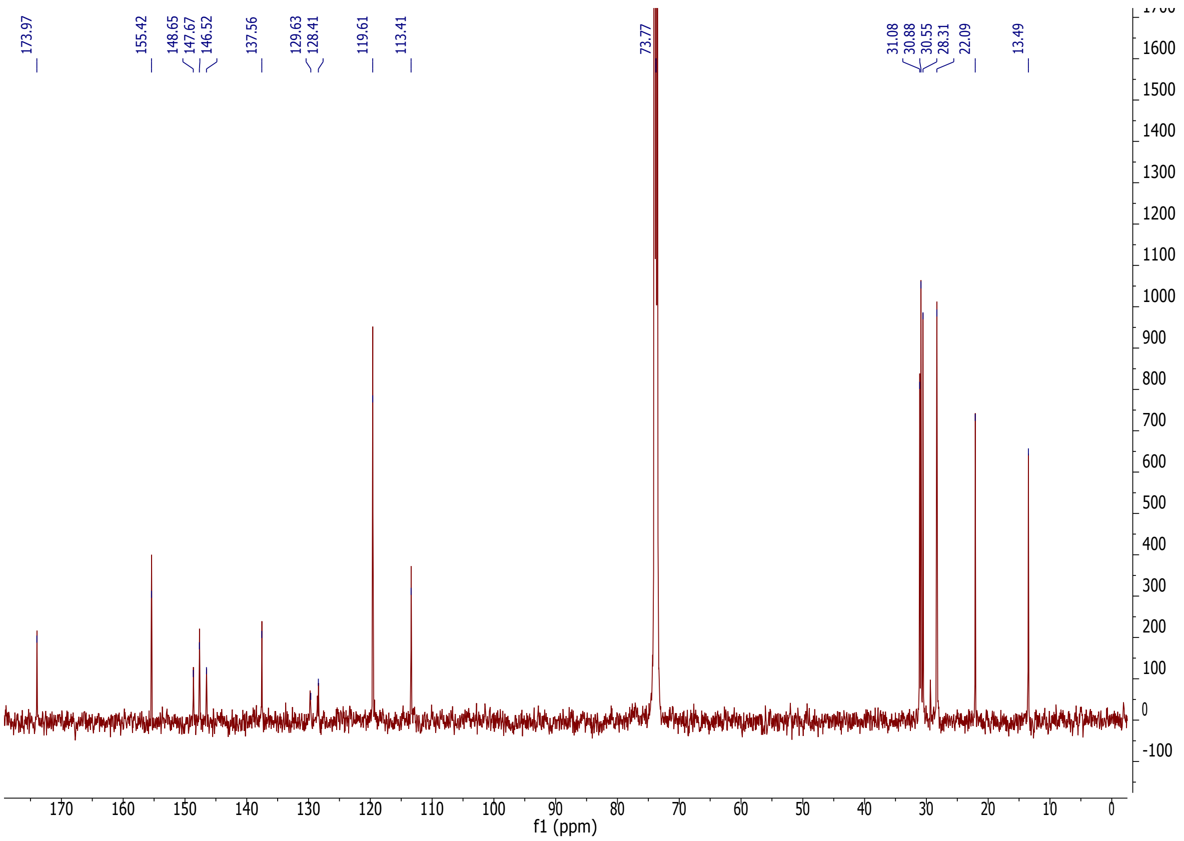

Figure S3: *^{13}C NMR of 2,2'-(5,10-difluoro-2,7-dihexyl-s-indaceno[1,2-b:5,6-b']dithiophene-4,9-diylidene)dicyanoimine* *(**2,7-dihexyl-diFIDT-di(N(CN))**) in TCE-d_2 at 120 °C*.

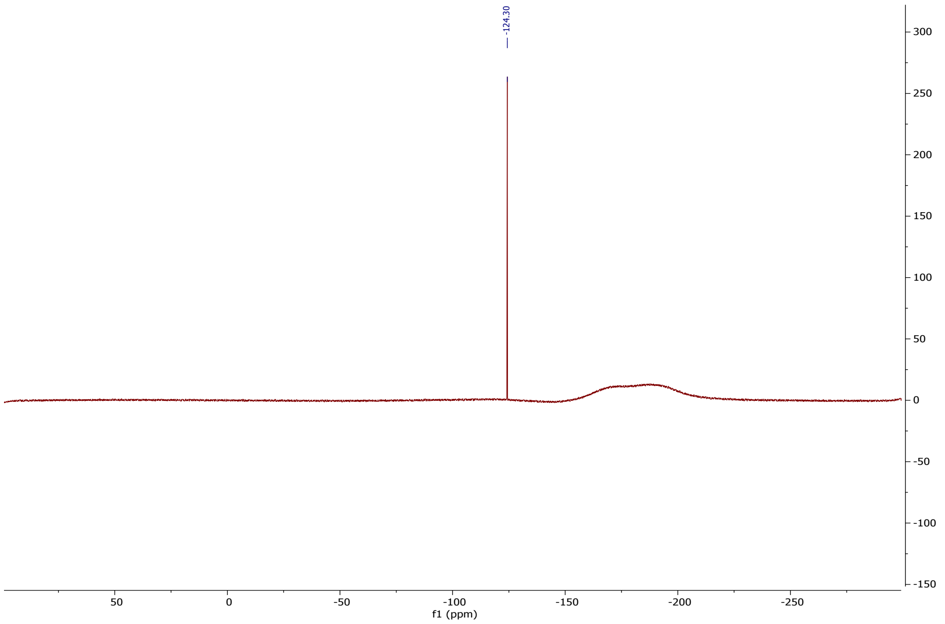

Figure S4: *^{19}F NMR of 2,2'-(5,10-difluoro-2,7-dihexyl-s-indaceno[1,2-b:5,6-b']dithiophene-4,9-diylidene)dicyanoimine* *(**2,7-dihexyl-diFIDT-di(N(CN))**) in $CDCl_3$.*

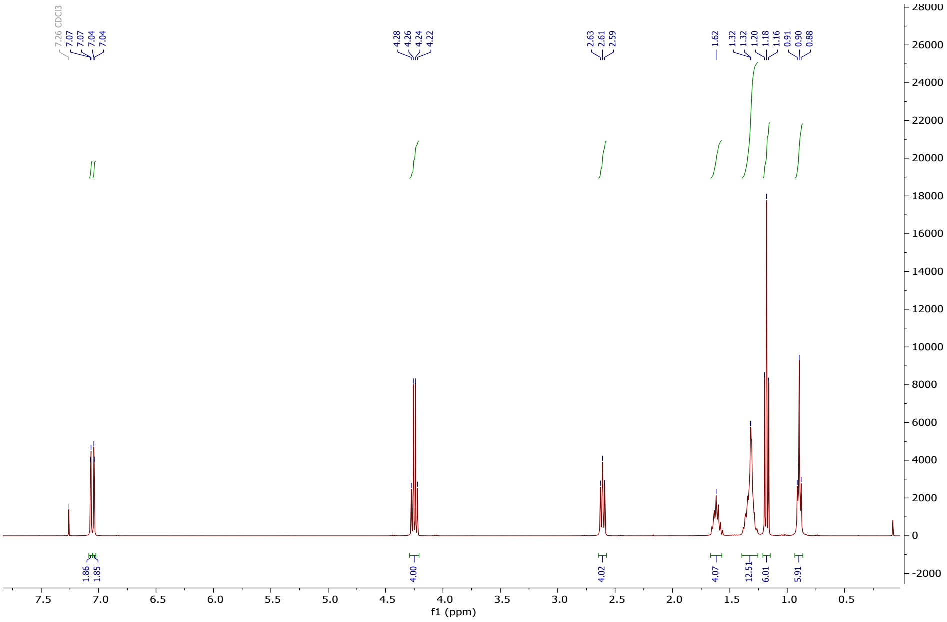

Figure S5: *^{1}H NMR of diethyl 2,5-difluoro-3,6-bis(4-hexylthiophen-2-yl)terephthalate* ***[3]*** *in $CDCl_3$.*

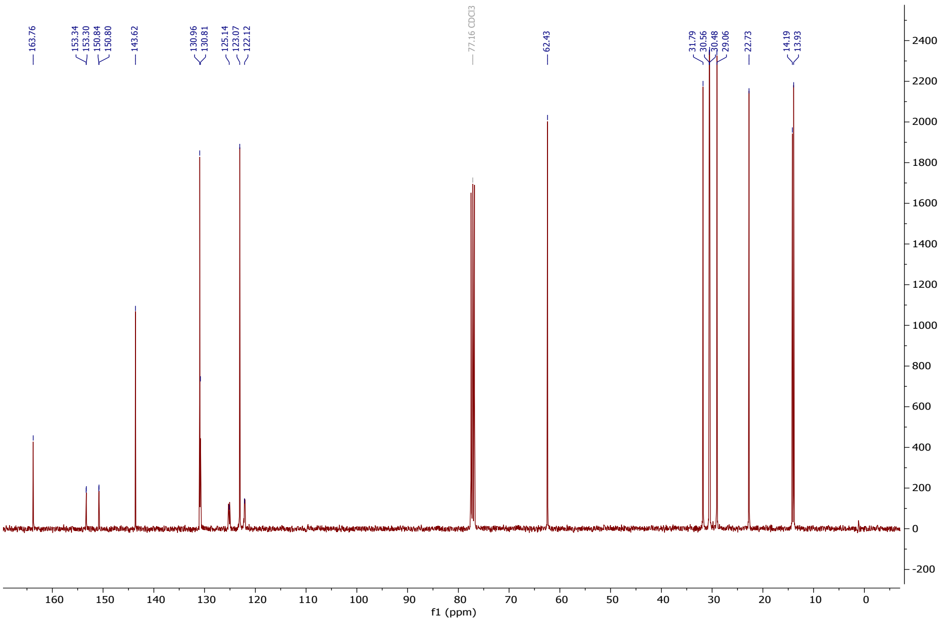

Figure S6: *^{13}C NMR of diethyl 2,5-difluoro-3,6-bis(4-hexylthiophen-2-yl)terephthalate* ***[3]*** *in $CDCl_3$.*

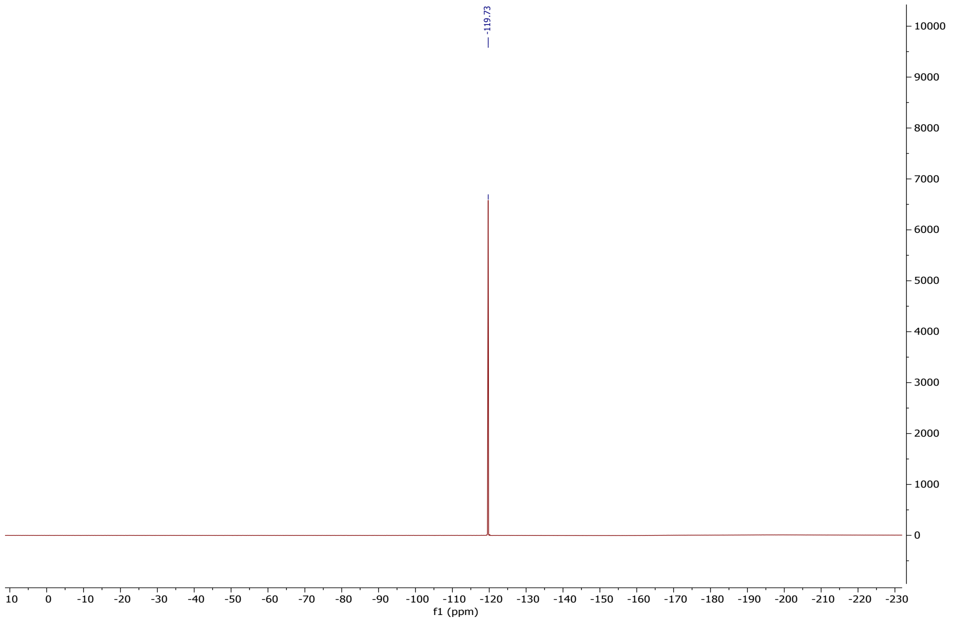

Figure S7: *^{19}F NMR of diethyl 2,5-difluoro-3,6-bis(4-hexylthiophen-2-yl)terephthalate* ***[3]*** *in $CDCl_3$.*

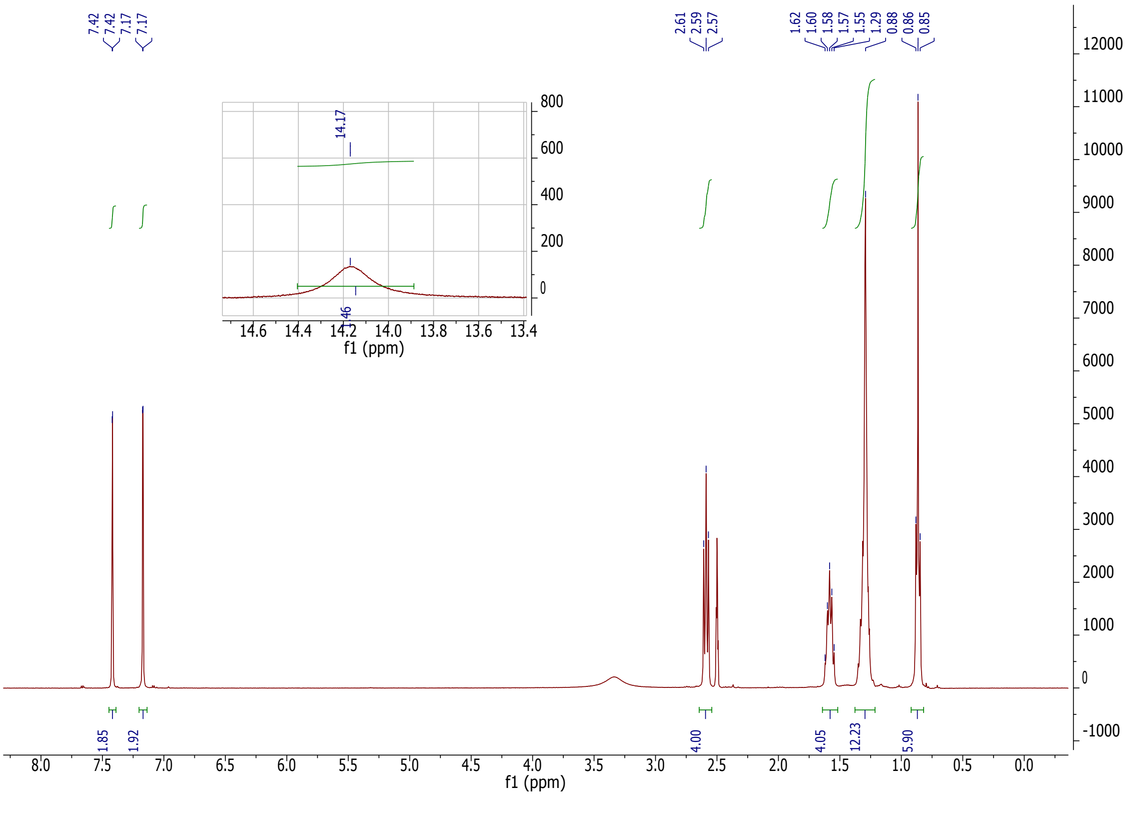

Figure S8: *^{1}H NMR of 2,5-bis(4-hexylthiophen-2-yl)-3,6-difluoroterephthalic acid* ***[4]*** *in DMSO-d_6.*

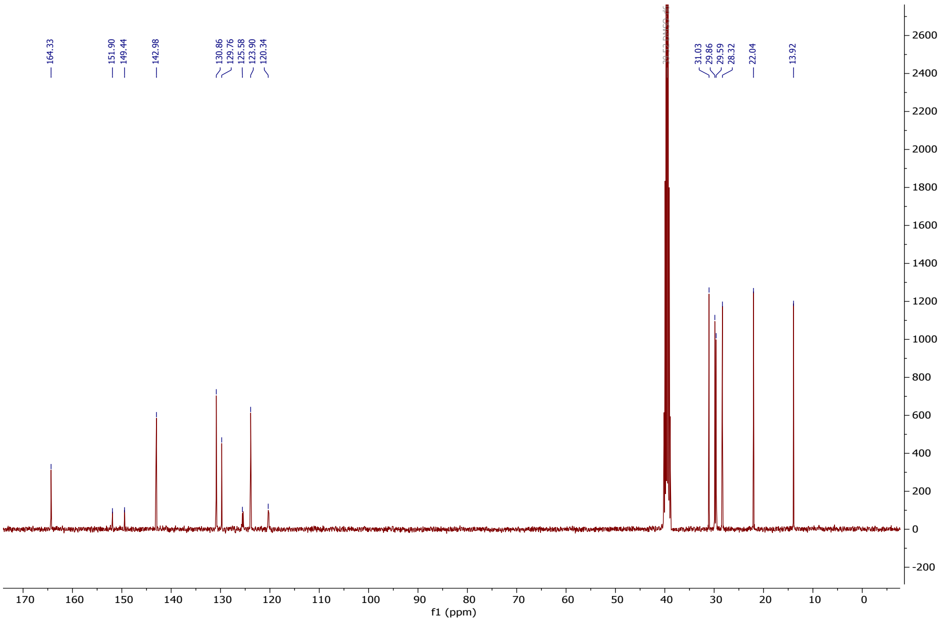

Figure S9: *^{13}C NMR of 2,5-bis(4-hexylthiophen-2-yl)-3,6-difluoroterephthalic acid **[4]** in DMSO-d_6.*

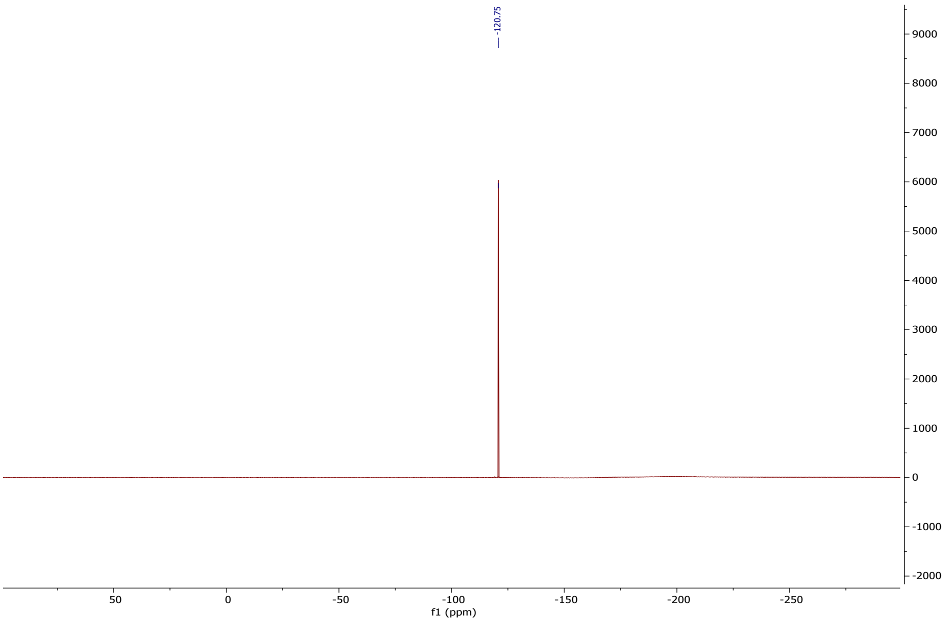

Figure S10: *^{19}F NMR of 2,5-bis(4-hexylthiophen-2-yl)-3,6-difluoroterephthalic acid **[4]** in DMSO-d_6.*

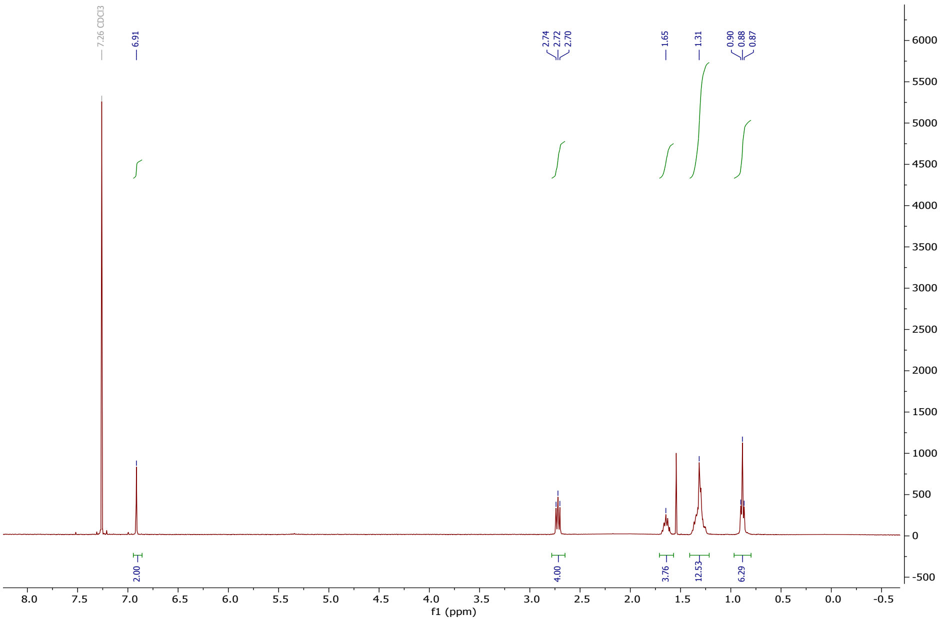

Figure S11: *^{1}H NMR of 3,8-dihexyl-5,10-difluoro-s-indaceno[1,2-b:5,6-b']dithiophene-4,9-dione* ***(3,8-dihexyl-diFIDT-di(O))*** *in $CDCl_3$.*

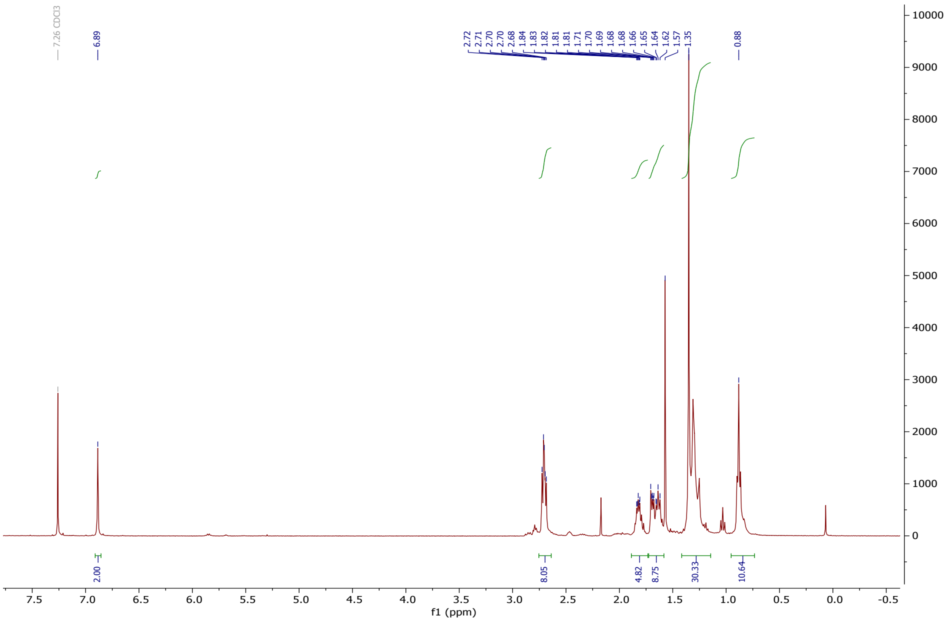

Figure S12: *^{1}H NMR of isolated side-product from Friedel-Crafts cyclisation of 3,8-dihexyl-diFIDT-di(O) in $CDCl_3$.*

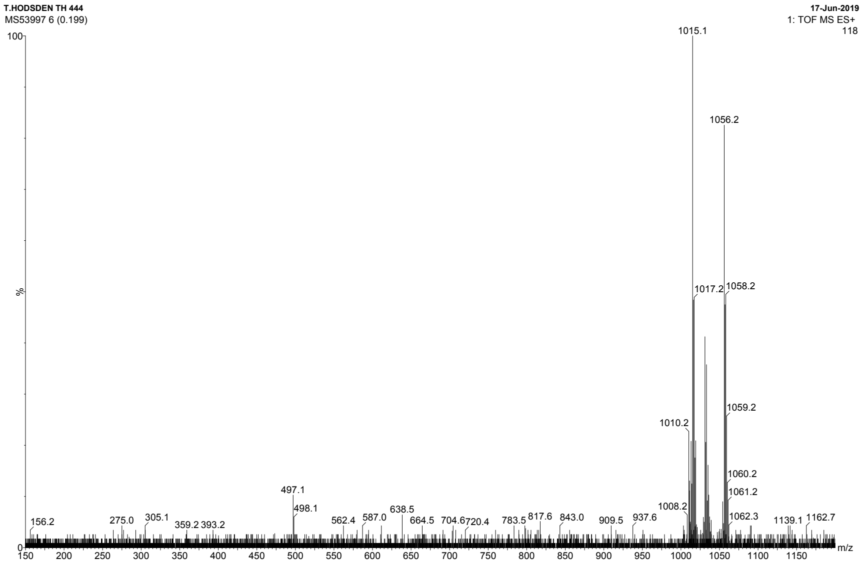

Figure S13: *TOF-ES MS of isolated side-product from Friedel-Crafts cyclisation 3,8-dihexyl-diFIDT-di(O).*

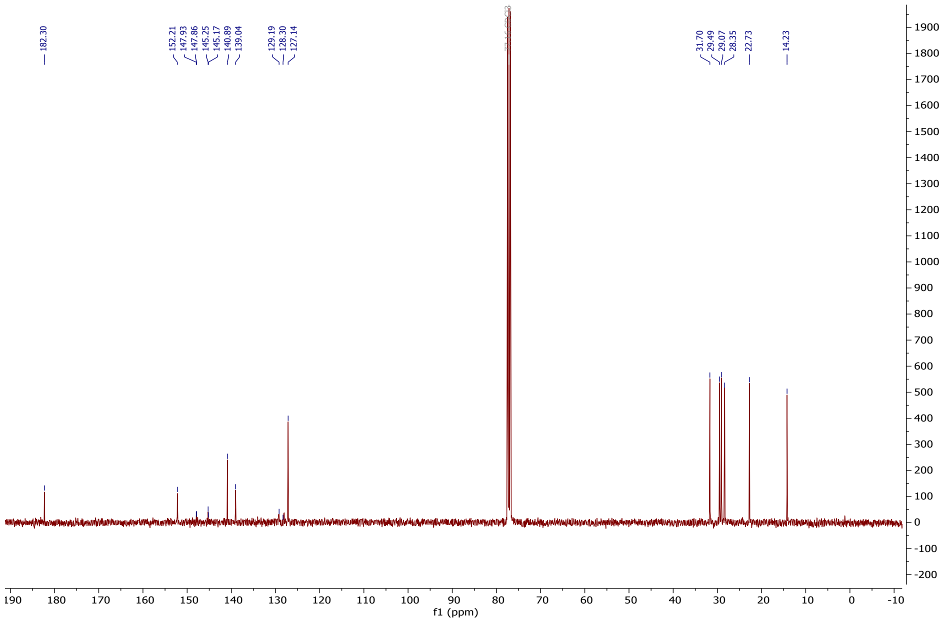

Figure S14: *^{13}C NMR of 3,8-dihexyl-5,10-difluoro-s-indaceno[1,2-b:5,6-b']dithiophene-4,9-dione (**3,8-dihexyl-diFIDT-di(O)**) in CDCl$_3$.*

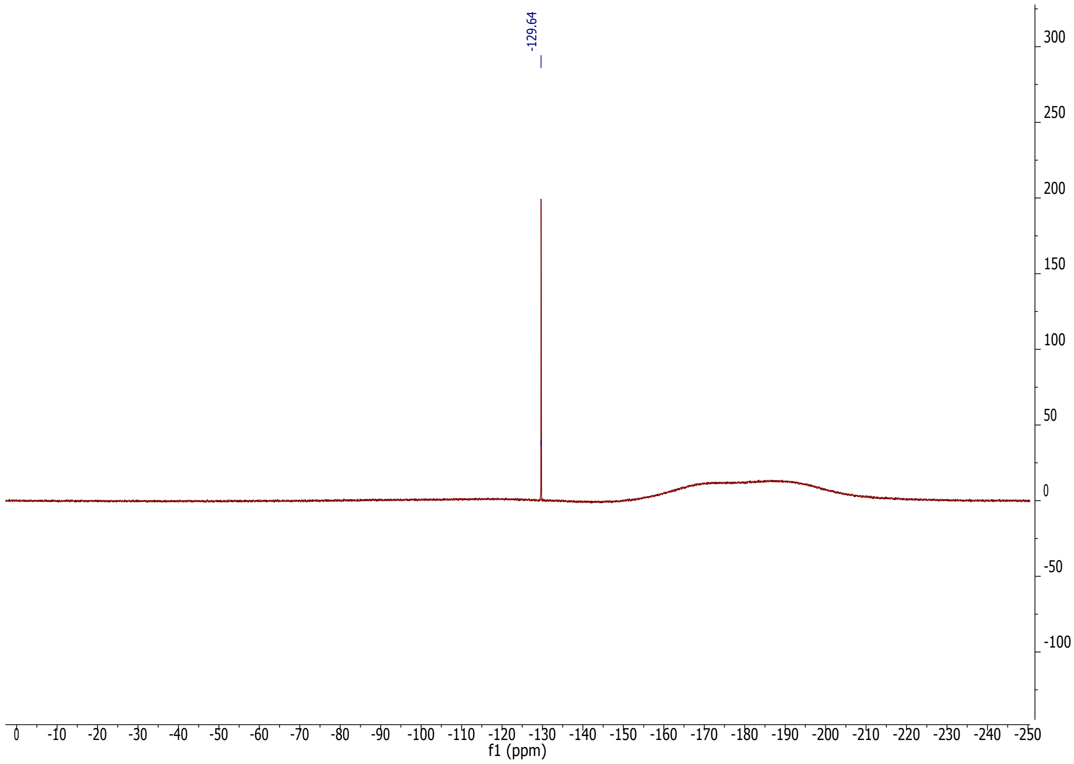

Figure S15: *^{19}F NMR of 3,8-dihexyl-5,10-difluoro-s-indaceno[1,2-b:5,6-b']dithiophene-4,9-dione* ***(3,8-dihexyl-diFIDT-di(O))*** *in $CDCl_3$.*

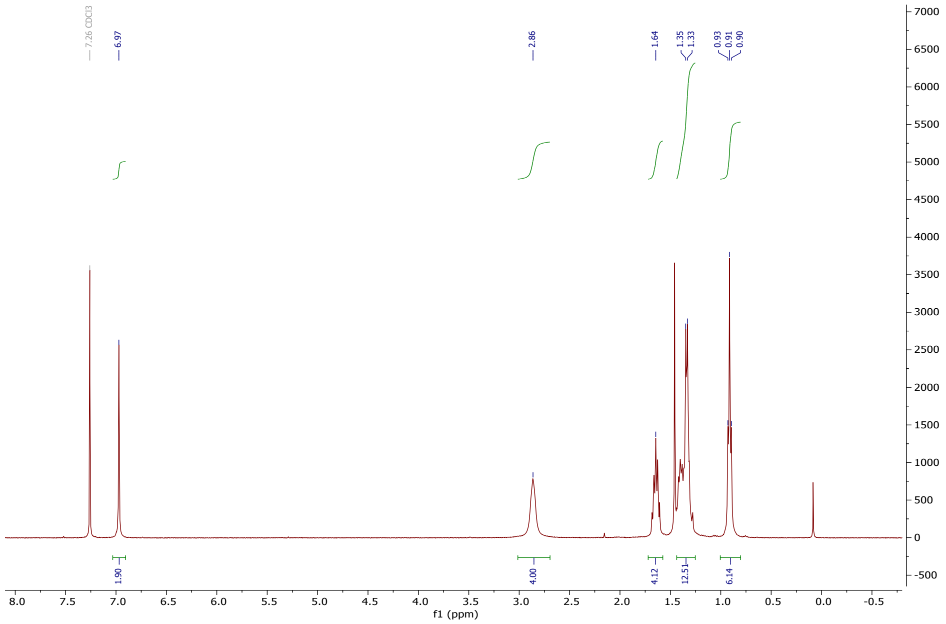

Figure S16: *^{1}H NMR of 2,2'-(5,10-difluoro-3,8-dihexyl-s-indaceno[1,2-b:5,6-b']dithiophene-4,9-diylidene)dicyanoimine* ***(3,8-dihexyl-diFIDT-di(N(CN)))*** *in $CDCl_3$ at 50 °C.*

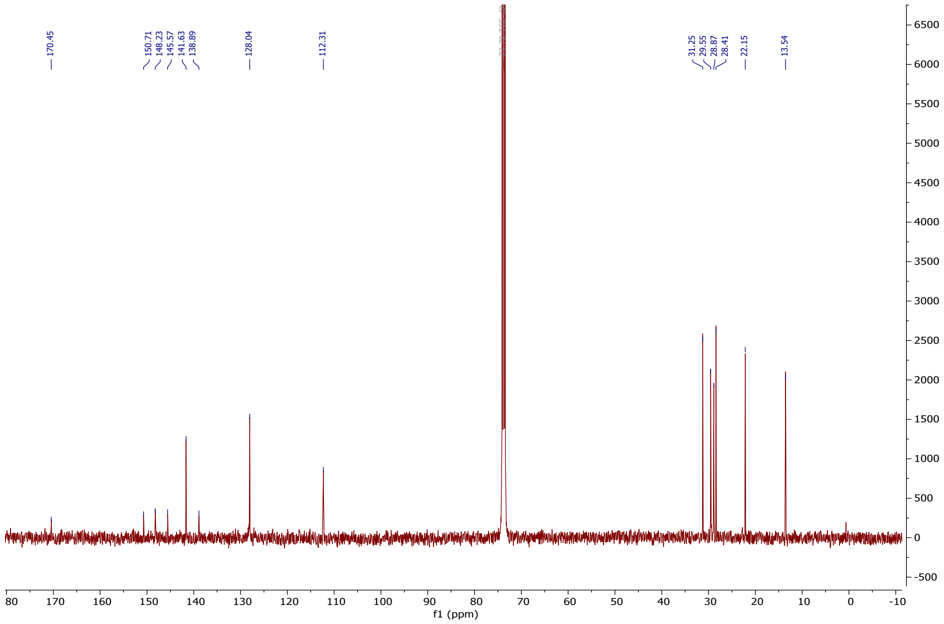

Figure S17: *^{13}C NMR of 2,2'-(5,10-difluoro-3,8-dihexyl-s-indaceno[1,2-b:5,6-b']dithiophene-4,9-diylidene)dicyanoimine **(3,8-dihexyl-diFIDT-di(N(CN)))** in TCE-d_2 at 120 °C.*

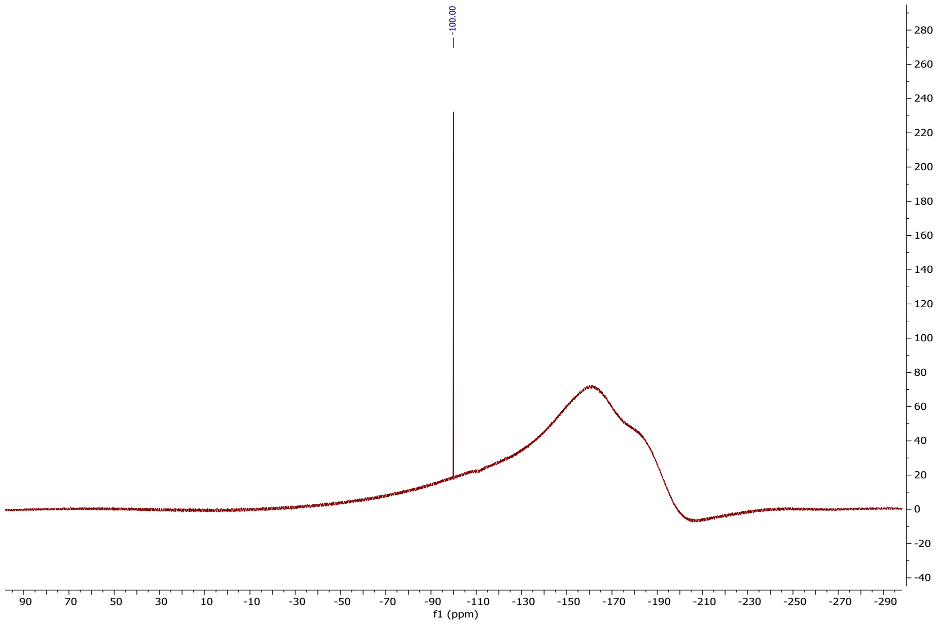

Figure S18: *^{19}F NMR of 2,2'-(5,10-difluoro-3,8-dihexyl-s-indaceno[1,2-b:5,6-b']dithiophene-4,9-diylidene)dicyanoimine **(3,8-dihexyl-diFIDT-di(N(CN)))** in CDCl$_3$ at 50 °C.*

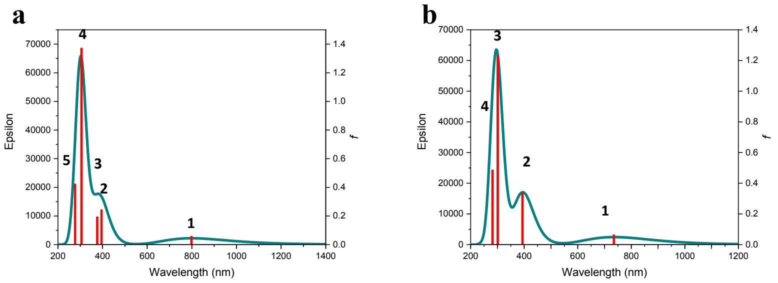

a)

1. HOMO→LUMO, 798 nm, *f* = 0.055
2. HOMO-4→LUMO, 395 nm, *f* = 0.240
   HOMO-2→LUMO
   HOMO→LUMO+2
3. HOMO-4→LUMO, 378 nm, *f* = 0.190
   HOMO-2→LUMO
   HOMO-1→LUMO+1
4. HOMO-7→LUMO, 306 nm, *f* = 1.369
   HOMO-4→LUMO
   HOMO-2→LUMO
   HOMO→LUMO+2
5. HOMO-7→LUMO, 277 nm, *f* = 0.420
   HOMO-3→LUMO+1
   HOMO-1→LUMO+1
   HOMO→LUMO+2

b)

1. HOMO→LUMO, 736 nm, *f* = 0.061
2. HOMO-4→LUMO, 393 nm, *f* = 0.336
   HOMO-2→LUMO
   HOMO→LUMO+2
3. HOMO-7→LUMO, 301 nm, *f* = 1.227
   HOMO-4→LUMO
   HOMO-3→LUMO+1
   HOMO→LUMO+2
4. HOMO-7→LUMO, 282 nm, *f* = 0.483
   HOMO-3→LUMO+1
   HOMO→LUMO+2

Figure S19: *Predicted UV-Vis spectra from TD-DFT energy calculations of a)* ***2,7-dialkyl-diFIDT-di(N(CN))*** *and b)* ***3,8-dialkyl-diFIDT-di(N(CN))*** *after geometry optimisation with DFT B3LYP/6-311+G(d,p), with selected excitations highlighted.*

The X-ray crystal structure of 2,7-dihexyl-diFIDT-di(N(CN))

Crystal data for **2,7-dihexyl-diFIDT-di(N(CN))**: $C_{30}H_{28}F_2N_4S_2$, M = 546.68, monoclinic, $P2_1/n$ (no. 14), a = 4.70133(12), b = 16.7253(7), c = 16.7198(5) Å, β = 97.105(2)°, V = 1304.60(7) Å^3, Z = 2 [C_i symmetry], D_c = 1.392 g cm^{-3}, μ(Cu-Kα) = 2.199 mm^{-1}, T = 173 K, black platy needles, Agilent Xcalibur PX Ultra A diffractometer; 4504 independent measured reflections (R_{int} = 0.0332), F^2 refinement,[3,4] R_1(obs) = 0.0538, wR_2(all) = 0.2202, 3845 independent observed absorption-corrected reflections [$|F_o| > 4\sigma(|F_o|)$, completeness to θ_{full}(67.7°) = 99.9%], 174 parameters. CCDC 2050898.

The crystal of **2,7-dihexyl-diFIDT-di(N(CN))** that was studied was found to be a two component twin in a *ca*. 54:46 ratio, with the two lattices related by the approximate twin law [–1.00 0.00 0.0 0.00 –1.00 0.00 0.88 0.00 1.00]. The structure was found to sit across a centre of symmetry situated at the middle of the C_6F_2 ring.

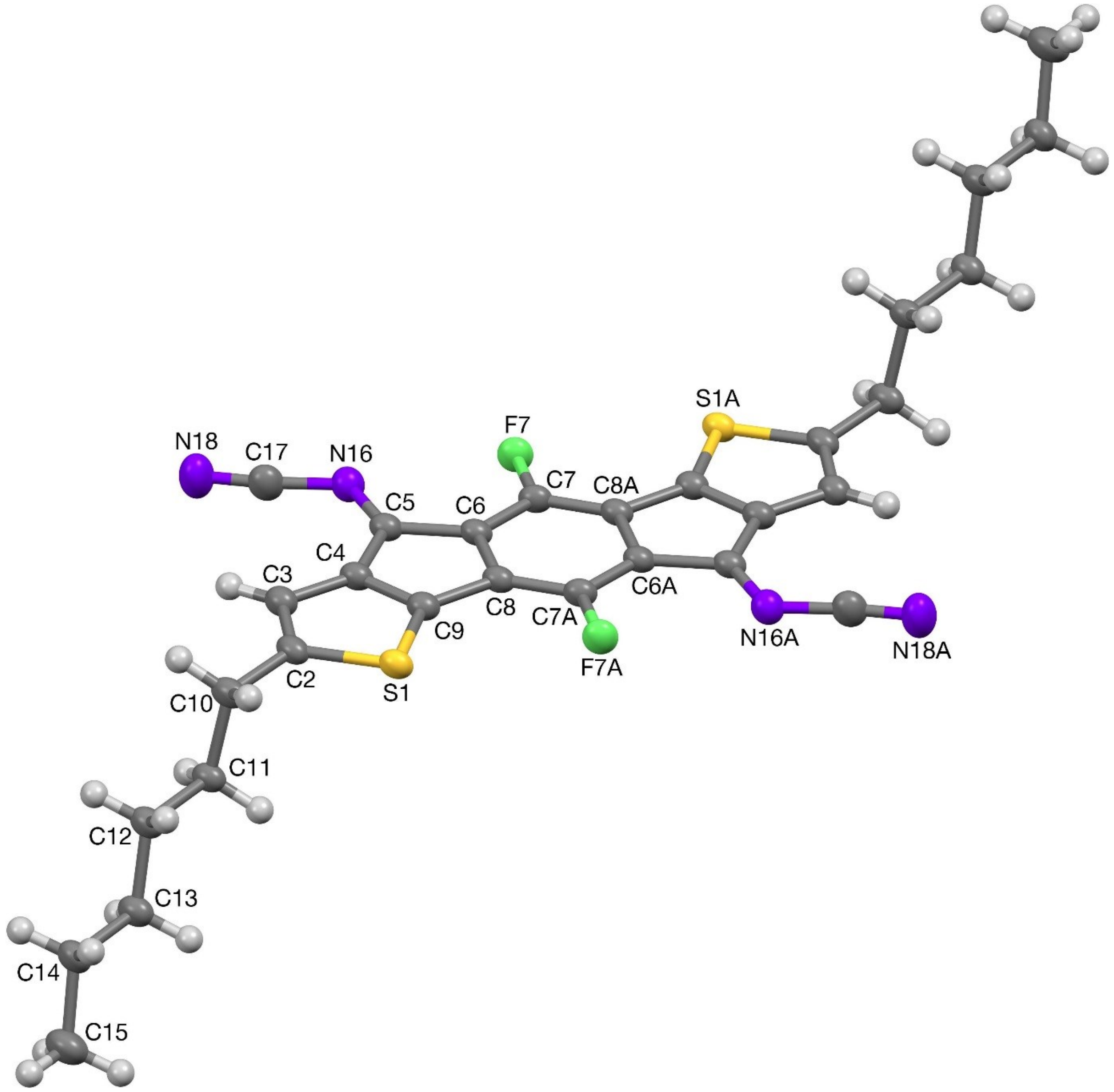

Figure S20: *The crystal structure of* ***2,7-dihexyl-diFIDT-di(N(CN))*** *(50% probability ellipsoids). The molecule sits across a centre of symmetry at the middle of the central* C_6F_2 *ring.*

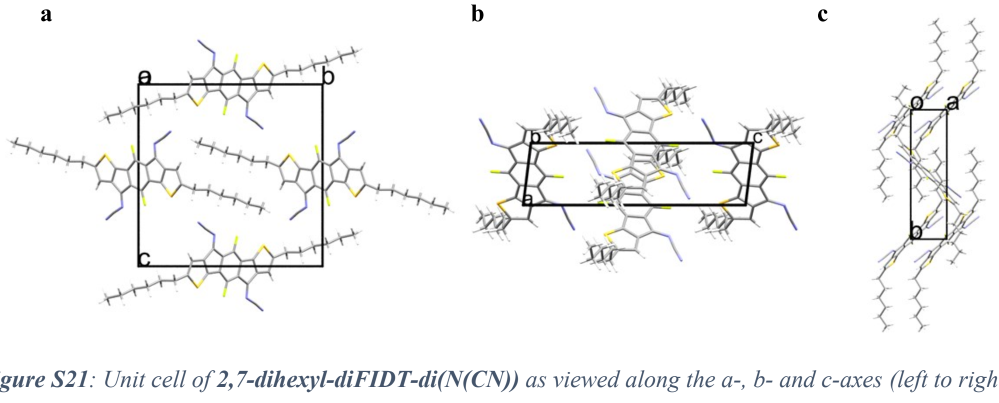

Figure S21: *Unit cell of* ***2,7-dihexyl-diFIDT-di(N(CN))*** *as viewed along the a-, b- and c-axes (left to right).*

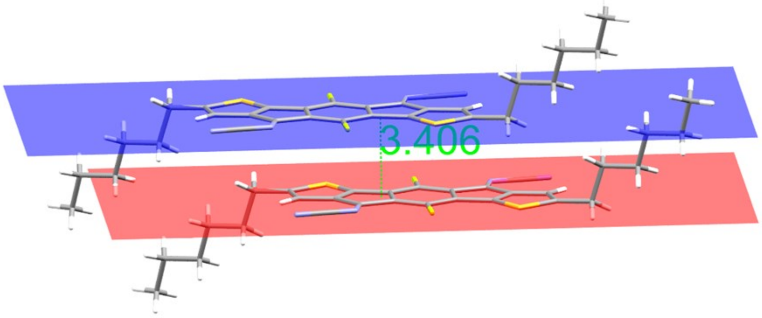

Figure S22: Interlayer spacing of ***2,7-dihexyl-diFIDT-di(N(CN))***

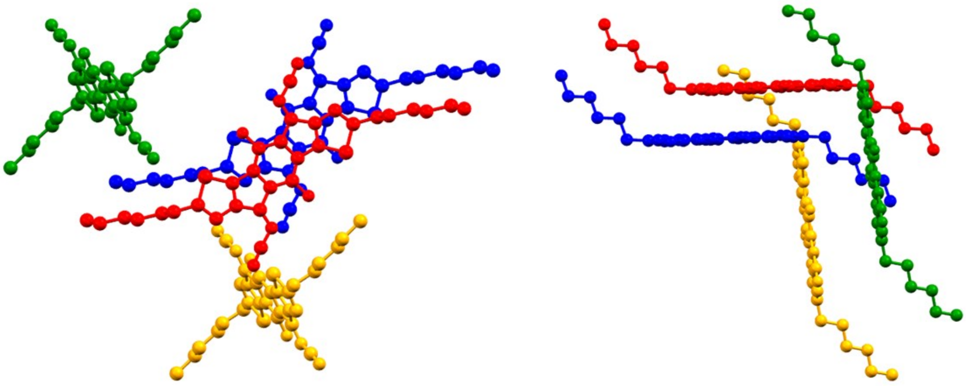

2,7-dihexyl-diFIDT-di(N(CN)) Crystal	X	ES	EX	IND	DISP	TOT
Blue/Green	H	-3.79	4.59	-1.23	-4.71	-5.15
Blue/Green	F	-3.95	4.53	-1.20	-4.72	-5.34
Blue/Orange	H	-1.54	2.87	-0.55	-4.89	-4.11
Blue/Orange	F	-2.12	3.65	-0.60	-5.41	-4.47
Blue/Red	H	-10.59	33.22	-3.52	-49.03	-29.92
Blue/Red	F	-8.12	32.43	-3.78	-49.04	-28.50

Figure S23: *SAPT0 energies for selective dimers of* ***2,7-dihexyl-IDT-di(N(CN))*** *and* ***2,7-dihexyl-diFIDT-di(N(CN))*** *in the* ***2,7-dihexyl-diFIDT-di(N(CN))*** *crystal packing motif.*

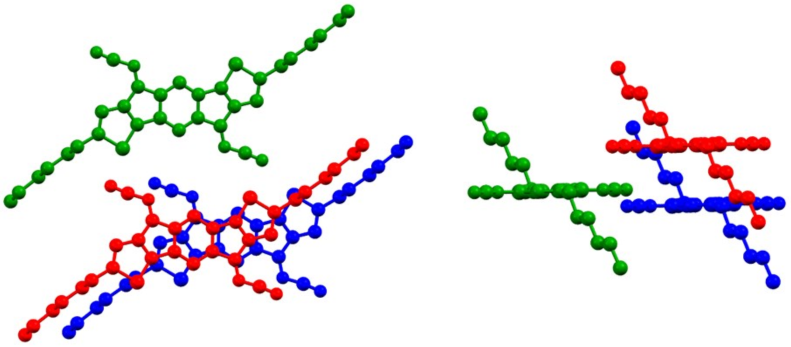

2,7-dihexyl-IDT-di(N(CN)) Crystal	X	ES	EX	IND	DISP	TOT
Blue/Green	H	-5.43	6.96	-1.73	-7.93	-8.13
Blue/Green	F	-8.68	22.20	-2.84	-10.48	0.20
Red/Green	H	-6.08	8.89	-2.86	-8.45	-8.49
Red/Green	F	-5.97	6.96	-1.78	-8.18	-8.97
Blue/Red	H	-8.98	28.89	-3.18	-45.15	-28.43
Blue/Red	F	-6.72	28.36	-3.41	-45.18	-26.95

Figure S24: *SAPT0 energies for selective dimers of* ***2,7-dihexyl-IDT-di(N(CN))*** *and* ***2,7-dihexyl-diFIDT-di(N(CN))*** *in the* ***2,7-dihexyl-IDT-di(N(CN))*** *crystal packing motif.*

The X-ray crystal structure of 3,8-dihexyl-diFIDT-di(N(CN))

Crystal data for **3,8-dihexyl-diFIDT-di(N(CN))**: $C_{30}H_{28}F_2N_4S_2$, M = 546.68, triclinic, P-1 (no. 2), a = 4.6926(6), b = 8.4797(19), c = 17.028(3) Å, α = 78.265(17), β = 88.149(12), γ = 75.301(14)°, V = 641.6(2) Å^3, Z = 1 [C_i symmetry], D_c = 1.415 g cm^{-3}, μ(Cu-Kα) = 2.236 mm^{-1}, T = 173 K, dark green needles, Agilent Xcalibur PX Ultra A diffractometer; 2401 independent measured reflections (R_{int} = 0.0628), F^2 refinement,[3,4] R_1(obs) = 0.0652, wR_2(all) = 0.1839, 1767 independent observed absorption-corrected reflections [$|F_o| > 4\sigma(|F_o|)$, completeness to θ_{full}(67.7°) = 96.5%], 173 parameters. CCDC 2050899.

The structure of **3,8-dihexyl-diFIDT-di(N(CN))** was found to sit across a centre of symmetry at the middle of the central C_6F_2 ring.

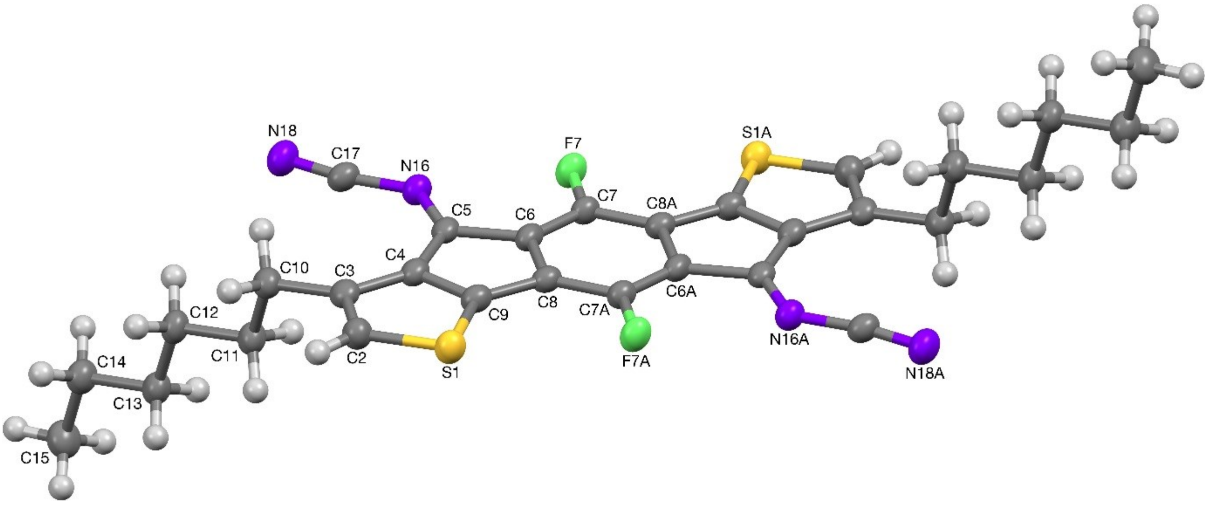

***Figure S25**: The crystal structure of **3,8-dihexyl-diFIDT-di(N(CN))** (50% probability ellipsoids). The molecule sits across a centre of symmetry at the middle of the central C_6F_2 ring.*

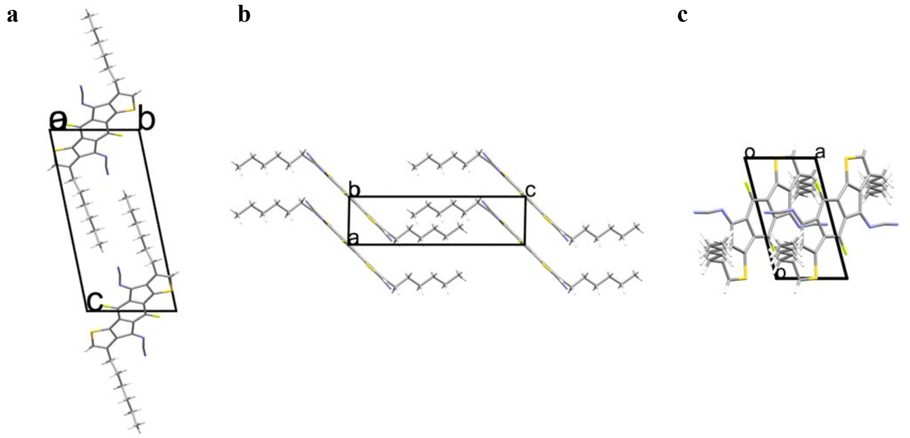

***Figure S26**: Unit cell of **3,8-dihexyl-diFIDT-di(N(CN))** as viewed along the a-, b- and c-axes (left to right).*

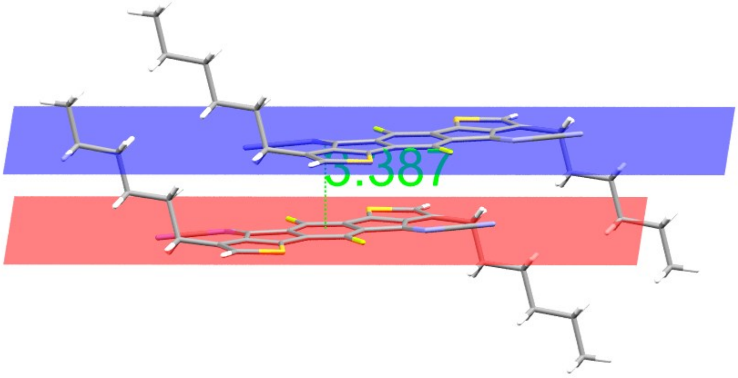

***Figure S27**: Interlayer spacing of **3,8-dihexyl-diFIDT-di(N(CN))**.*

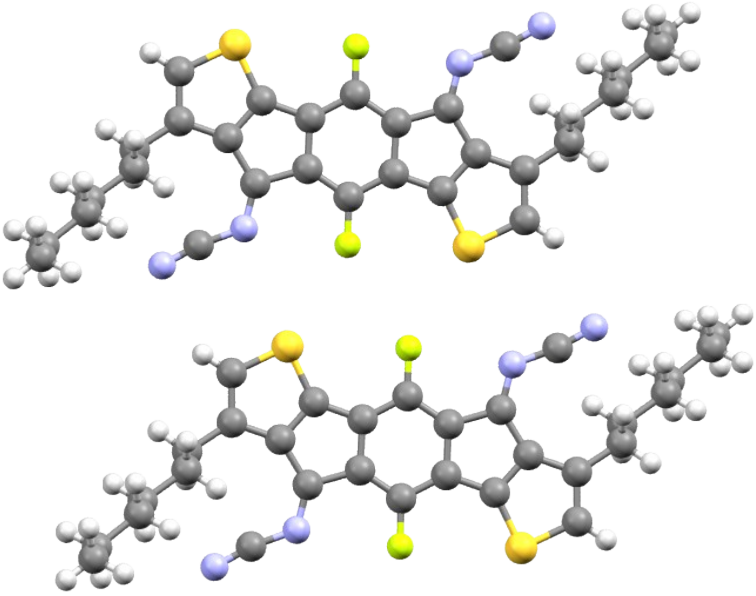

X	ES	EX	IND	DISP	TOT
F	-5.91	6.85	-1.76	-8.80	-9.61
H	-4.87	5.47	-1.50	-8.05	-8.95

***Figure S28:** SAPT0 energies (in kcal/mol) for in-plane dimers of **3,8-dihexyl-diFIDT-di(N(CN))** and its non-fluorinated analogue in the **3,8-dihexyl-diFIDT-di(N(CN))** crystal packing motif.*

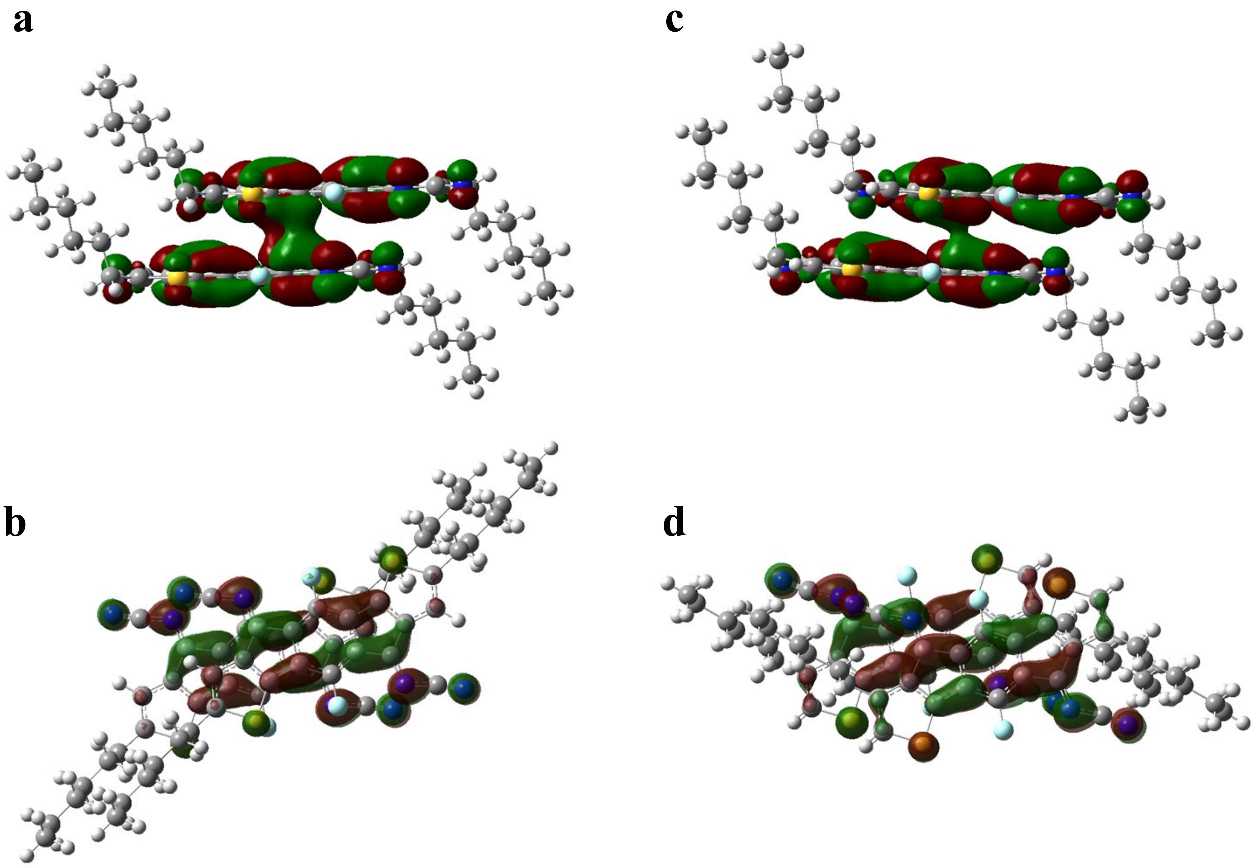

Figure S29*: Representative LUMO – LUMO interactions for molecular pairs from the crystal structures of* ***2,7-dihexyl-diFIDT-di(N(CN))*** *(a & b) and* ***3,8-dihexyl-diFIDT-di(N(CN))*** *(c & d), calculated using B3LYP/6-31G(d)) following the approach of Valeev et al*[2]*. a & c) Side-view, highlighting extent of LUMO delocalisation across the molecular pair. b & d) Top-view, highlighting the different relative displacements.*

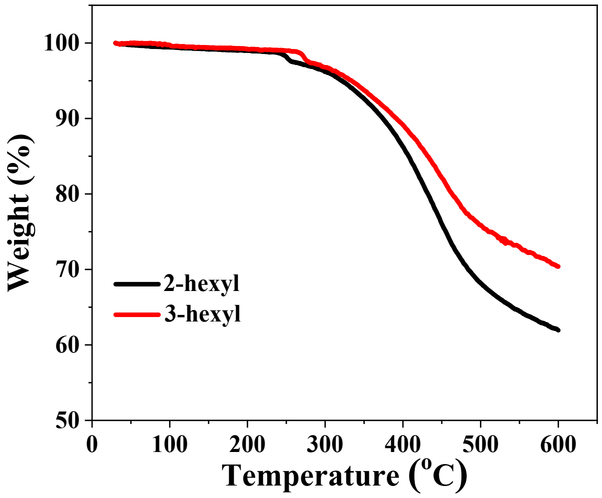

Figure ***S30****: TGA plots for* ***2,7-dihexyl-diFIDT-di(N(CN))*** *(black) and* ***3,8-dihexyl-diFIDT-di(N(CN))*** *(red).*

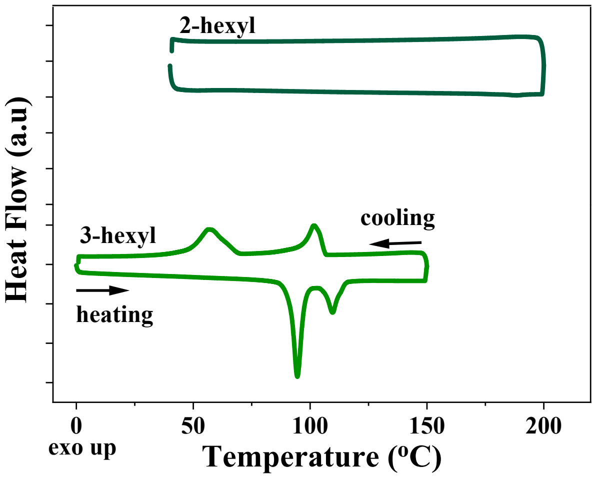

*Figure **S31**: DSC plots (1st Cycle) for **2,7-dihexyl-diFIDT-di(N(CN))** (top) and **3,8-dihexyl-diFIDT-di(N(CN))** (bottom).*

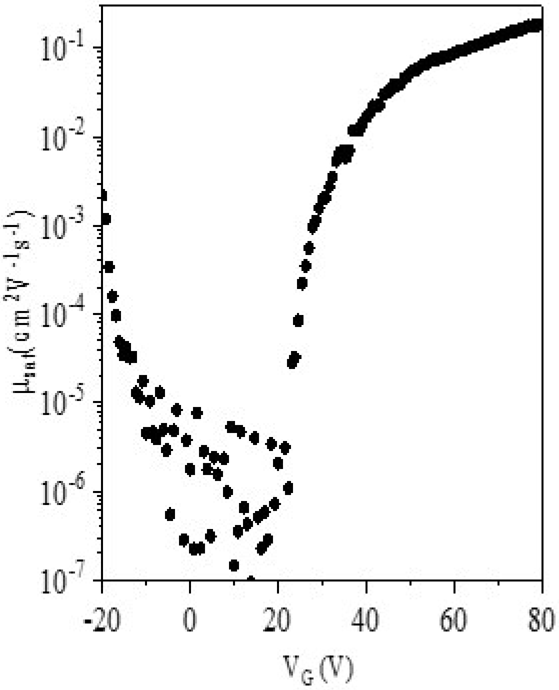

***Figure S32:** **E**lectron mobility measured in saturation, μ_{sat}, curves for blade-coated BC-TG devices of **2,7-dihexyl-diFIDT-di(N(CN))** after annealing at 200 °C (transfer and output plots shown in figure 6)*

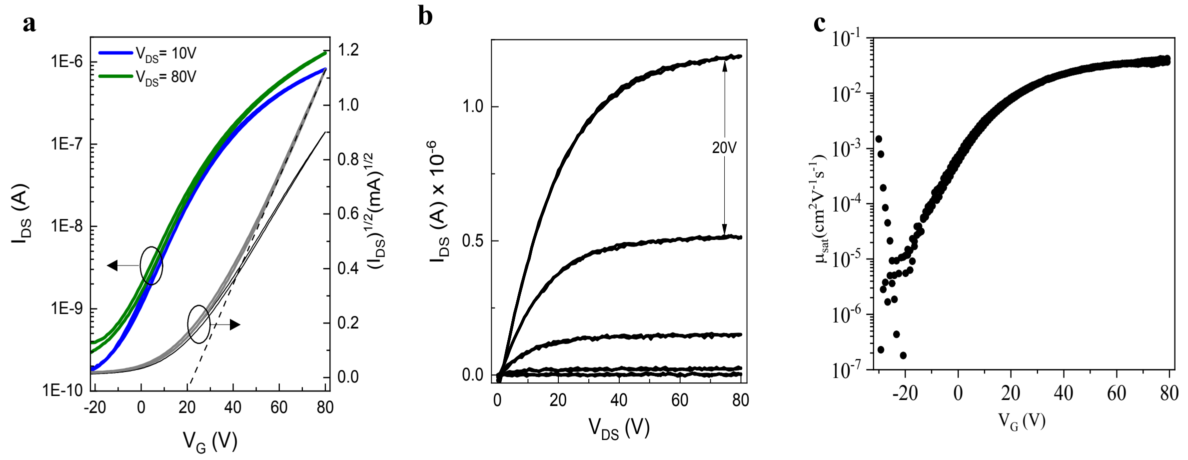

Figure S33: *Transfer (a), output (b) and electron mobility measured in saturation, μ_{sat}, curves for blade-coated BC-TG devices of **3,8-dihexyl-diFIDT-di(N(CN))**.*

References

[1] T. Hodsden, K. J. Thorley, J. Panidi, A. Basu, A. V. Marsh, H. Dai, A. J. P. White, C. Wang, W. Mitchell, F. Glöcklhofer, T. D. Anthopoulos, M. Heeney, *Adv. Funct. Mater.* **2020**.

[2] E. F. Valeev, V. Coropceanu, D. A. Da Silva Filho, S. Salman, J. L. Brédas, *J. Am. Chem. Soc.* **2006**, *128*, 9882.

[3] SHELXTL v5.1, Bruker AXS, Madison, WI, 1998.

[4] SHELX-2013, G.M. Sheldrick, *Acta Cryst.*, 2015, **C71**, 3-8